BIOTECHNOLOGY
BIOENGINEERING WILEY

S-adenosylmethionine and methylthioadenosine boost cellular productivities of antibody forming Chinese hamster ovary cells

Natascha Verhagen[1] 🔘 | Attila Teleki[1] | Christoph Heinrich[2] | Martin Schilling[3] | Andreas Unsöld[4] | Ralf Takors[1] 🔘

[1]Institute of Biochemical Engineering, University of Stuttgart, Allmandring, Stuttgart, Germany

[2]Xell AG, Bielefeld, Germany

[3]Evonik Nutrition & Care GmbH, Darmstadt, Germany

[4]Boehringer Ingelheim Pharma GmbH & Co. KG, Biberach, Germany

Correspondence
Ralf Takors, Institute of Biochemical Engineering, University of Stuttgart, Allmandring 31, 70569 Stuttgart, Germany.
Email: ralf.takors@ibvt.uni-stuttgart.de

Funding information
Bundesministerium für Bildung und Forschung, Grant/Award Number: 031L0077A

Abstract

The improvement of cell specific productivities for the formation of therapeutic proteins is an important step towards intensified production processes. Among others, the induction of the desired production phenotype via proper media additives is a feasible solution provided that said compounds adequately trigger metabolic and regulatory programs inside the cells. In this study, S-(5′-adenosyl)-L-methionine (SAM) and 5′-deoxy-5′-(methylthio)adenosine (MTA) were found to stimulate cell specific productivities up to approx. 50% while keeping viable cell densities transiently high and partially arresting the cell cycle in an anti-IL-8-producing CHO-DP12 cell line. Noteworthy, MTA turned out to be the chemical degradation product of the methyl group donor SAM and is consumed by the cells.

KEYWORDS
5′-deoxy-5′-(methylthio)adenosine (MTA), cell cycle arrest, cell specific productivity, Chinese hamster ovary (CHO) cell, medium optimization, S-(5′-adenosyl)-L-methionine (SAM)

1 | INTRODUCTION

Therapeutic proteins such as monoclonal antibodies (mAB) dominate the global market for biopharmaceuticals and are mostly produced in Chinese hamster ovary (CHO) cells (Walsh, 2018). The last decades of biomanufacturing witnessed a steady rise of product titers in conventional fed-batch modes reaching 5–8 g/L in 12–14 days process time (Reinhart, Damjanovic, Kaisermayer, & Kunert, 2015; Schaub et al., 2010; Wurm, 2004). However, those volumetric productivity improvements predominately mirror elevated viable cell densities rather than the equal rise of cell specific productivities (CSPs). The latter however, is of outstanding importance when the next generation of intensified bioprocesses should be realized, in particular when using perfusion processes (Becker, Junghans, Teleki, Bechmann, & Takors, 2019; Templeton, Smith, et al., 2017; Zhang et al., 2013).

Consequently, novel approaches are needed that boost CSPs for pharmaceutical proteins. As a prerequisite, detailed understanding of the roles of interacting partners in the complex regulatory patterns of CHO metabolism is necessary. As a result of this, novel switches to enhance CSPs may be derived. Promising studies focused on metabolism (Handlogten et al., 2018; Junghans et al., 2019; Templeton, Xu, Roush, & Chen, 2017), transcription (Pfizenmaier, Junghans, Teleki, & Takors, 2016; Sha, Bhatia, & Yoon, 2018), and on epigenetics. Epigenetic adaption mechanisms that is histone modification via acetylation and DNA methylation are basic features of CHO cell adaption. Nematpour et al. (2017) showed that stabilized acetylation by inhibition of histone deacetylases with medium additives enhanced mAB productivity in CHO cells. Furthermore, DNA methylation which links genetics with transcriptomics (Wippermann, Rupp, Brinkrolf, Hoffrogge, & Noll, 2015) was revealed to be the main

reason for particular downregulation and upregulation patterns found in high-producer cell lines (Feichtinger et al., 2016; Harreither et al., 2015). Recent studies of Dhiman et al. (2019) demonstrated that more than half of the analyzed nuclear genes are susceptible to methylation. Consequently, the addition of molecules interacting with epigenetic regulation mechanisms offers the intrinsic potential to improve CSPs.

In this context, the cosubstrate S-(5′-adenosyl)-L-methionine (SAM) was chosen as a medium additive whose structure was discovered in the early 1950s (Cantoni, 1951). SAM may be involved in aminopropylation (polyamine synthesis), trans-methylaton and -sulfuration underlining its crucial role for cellular growth and regulation. Accordingly, SAM limitation may affect gene expression, membrane fluidity, and glutathione availability reflecting its roles in DNA methylation, methylation of phospholipids, and trans-sulfuration, respectively (Finkelstein, 1990; Mato, Alvarez, Ortiz, & Pajares, 1997). Metabolically, the methyl group donor SAM is created by methionine adenosyltransferase (MAT) using adenosine triphosphate (ATP) and L-methionine as substrates. In CHO, the latter needs to be supplemented in the medium. In methylation reactions, SAM is de-methylated to S-(5′-adenosyl)-L-homocysteine (SAH) further de-adenylated to homocysteine, re-methylated to methionine, and finally re-adenosylated to SAM again (SAM cycle; Finkelstein, 1990; Mato et al., 1997). Accordingly, the cycle not only regenerates the key methyl donor SAM, it also provides important precursors: Homocysteine serves as a precursor for glutathione synthesis (Lu, 1998) which is an important antioxidant in cells. By analogy, SAM enters the polyamine synthesis (Finkelstein, 1990). Investigations on liver disease demonstrated that extracellular SAM influences the cellular glutathione level. Likely, SAM is taken up by the cells (Mato et al., 1997) which may explain why SAM-treated liver cells showed decreased growth rate, prevented the development of liver cancer (Cai, Mao, Hwang, & Lu, 1998; Pascale et al., 1993) and disclosed antiapoptotic mechanisms (Ansorena, 2002).

Summarizing, SAM is a crucial cosubstrate that serves as a key methyl donor thereby linking metabolism with cellular regulation and epigenetics. Consequently, it offers the intrinsic potential to function as an additive that boosts CSPs in CHO cells.

2 | MATERIALS AND METHODS

2.1 | Seed train, shake flask cultivation, and addition of SAM, 5′-deoxy-5′-(methylthio)adenosine (MTA), and L-homoserine lactone hydrochloride (HSL)

The following additives are products of Sigma-Aldrich (Steinheim, Germany): SAM, MTA, and HSL. The anti-IL-8-producing CHO-DP12 cell line (ATCC® CRL 12445™) adapted to grow in suspension was cultivated in chemically defined TC-42 medium (Xell AG, Bielefeld, Germany) supplemented with 4 mM L-glutamine (Carl Roth GmbH & Co. KG, Karlsruhe, Germany) and 200 nM methotrexate (Sigma-Aldrich, Steinheim, Germany). Seed train and experiments were performed in presterilized disposable shake flasks (Corning Inc., NY) in a humidified rotary shaker (Infors HT Minitron, Infors GmbH, Einsbach, Germany) at 37°C, 150 rpm with 50 mm displacement, and 5% CO_2. The additives SAM, MTA, and HSL were introduced after 48 hr of cultivation. In reference cell cultures, sterilized water was used to mimic the additional liquid volume in experimental cultures. Cultivation was performed with biological duplicates or quadruplicates.

2.2 | Extracellular analysis

Samples were taken at least once a day. Viable cell density, viability, and average cell diameter were determined using trypan blue staining using a Cedex XS cell counter (Innovatis AG, Bielefeld, Germany) for read out. The extracellular concentrations of D-glucose and L-lactate were determined using a Labotrace automatic analyzer (Trace Analytics GmbH, Braunschweig, Germany). The product concentration of immunoglobulin G (IgG) was determined applying enzyme-linked immunosorbent assay (ELISA; Pfizenmaier, Matuszczyk, & Takors, 2015). Each sampling and measurement procedure was performed in replicates.

2.3 | SAM and MTA determination

The amount of SAM and MTA was quantified on an Agilent 1200 Series HPLC system coupled with an Agilent 6410B triple quadrupole tandem mass spectrometer (QQQ-MS/MS; Agilent Technologies, Waldbronn, Germany). The LC-MS/MS method was based on a bicratic zwitterionic hydrophilic interaction chromatography (ZIC-pHILIC) under alkaline mobile phase conditions (10 mM ammonium acetate, pH 9.2) without prior derivatization (Feith, Teleki, Graf, Favilli, & Takors, 2019; Teleki, Sánchez-Kopper, & Takors, 2015). Targeted analytes were detected with high selectivity in multiple reaction monitoring (MRM) mode using pre-optimized precursor-to-product ion transitions and MS/MS parameters. Absolute quantification was performed by adapted standard-based external calibration with constant addition of global internal standards (L-norvaline and γ-aminobutyric acid) in diluted samples (1:8). Data were analyzed using MassHunter B.06.00 Analysis software.

2.4 | Cell cycle analysis

Cell cycle analysis was performed with an adapted method (Pfizenmaier-Wu, 2017). 10×10^6 cells were harvested and washed with ice-cold phosphate-buffered saline (PBS). After washing, the cells were immediately fixed with ice-cold fixation buffer (70% EtOH, 30% PBS [vol/vol]) and stored at −20°C until further analysis. The staining procedure started with gently thawing and resuspending of the cells. Then, cells were washed twice with PBS, resuspended in staining solution (propidium iodide and RNase A in PBS) and incubated for 10 min at 37°C in the dark. Samples stayed on ice until cell cycle analysis. The BD Accuri™ C6 Plus flow cytometer was used with 610/20 nm filter and detected 50,000 events per sample. Data were analyzed with BD Csampler software.

2.5 | Statistical methods

Error bars show standard deviations that were calculated based on four or two biological replicates (considering the technical replicates). Unpaired one-sided Student's t test was performed to investigate the data for statistical significance (***p = .001, **p = .01, *p = .05).

3 | RESULTS

3.1 | SAM addition boosted CSP while repressing growth

After 48 hr cultivation time, SAM was added reaching a concentration of 250 µM. Notably, REF received the equivalent volume of water to prevent any bias due to medium dilution. The SAM-treated cultures reduced maximum viable cell density (VCD) and growth rate (between 48 and 120 hr) by 10% and 18% compared with REF, respectively (Figure 1). However, high cell viabilities remained.

Although, SAM supplemented cells showed lower VCD than REF they reached more than 50% higher antibody titer (SAM: 192.73 ± 18.24 mg/L and REF: 123.39 ± 12.63 mg/L). The increased titer (>48 hr) transformed to increased CSP between 0 and 120 hr: SAM supplemented cells produced 9.81 ± 0.89 pg/day whereas the reference only showed 6.24 ± 0.51 pg/day. This corresponds to a 57% increase in CSP (Figure 2) after SAM addition.

3.2 | SAM degradation was not affected by the presence of cells

To investigate the effects of SAM addition and uptake extracellular SAM concentrations were monitored in the medium. The anticipated

SAM "uptake" coincided with equally fast degradation rates observed in cell-free cultivation medium under similar conditions (medium + SAM + cells, 11.54 ± 0.32 µM/hr; medium + SAM, 10.95 ± 0.30 µM/hr). Consequently, the direct cellular uptake of SAM seemed unlikely. To better understand SAM degradation, MTA as literature described degradation product was measured in the medium (Hoffman, 1986; Morana et al., 2002). Indeed, MTA was detectable in medium with and without cells but not in the reference (water addition). MTA concentration increased over time in medium without cells. In contrast, cell culture studies only showed high MTA levels at the beginning which decreased during the cultivation (Figure 3).

3.3 | SAM and its degradation products MTA and HSL

To check whether MTA is the inducer of the growth and IL-8 production phenotype, SAM and the degradation products MTA and HSL were studied in supplementation tests. The addition of substrates occurred after 48 hr of cultivation with a final concentration of 250 µM (REF was supplied with the same volume of water). The addition resulted in maximum VCDs (10^6 cells/ml) of SAM 7.085 ± 0.326, MTA 5.512 ± 0.203, HSL 8.216 ± 0.780, and REF 8.961 ± 0.576. As indicated in Figure 4, SAM and MTA supplementation caused reduced growth during 60–120 hr leading to a growth rate of 0.022 ± 0.002 hr^{-1} and 0.017 ± 0.001 hr^{-1}, respectively. However, there was no effect on the growth phenotype after HSL addition (0.028 ± 0.002 hr^{-1}) compared with the reference (0.028 ± 0.001 hr^{-1}).

Antibody titers were differently affected by the supplemented additives. Cultivations with SAM or MTA addition showed increased titers (SAM: 165.17 ± 7.53 mg/L and MTA: 167.72 ± 15.77 mg/L) whereas experiments with HSL (HSL: 125.94 ± 23.30 mg/L) and the reference (REF: 132.11 ± 9.61 mg/L) showed no improvements.
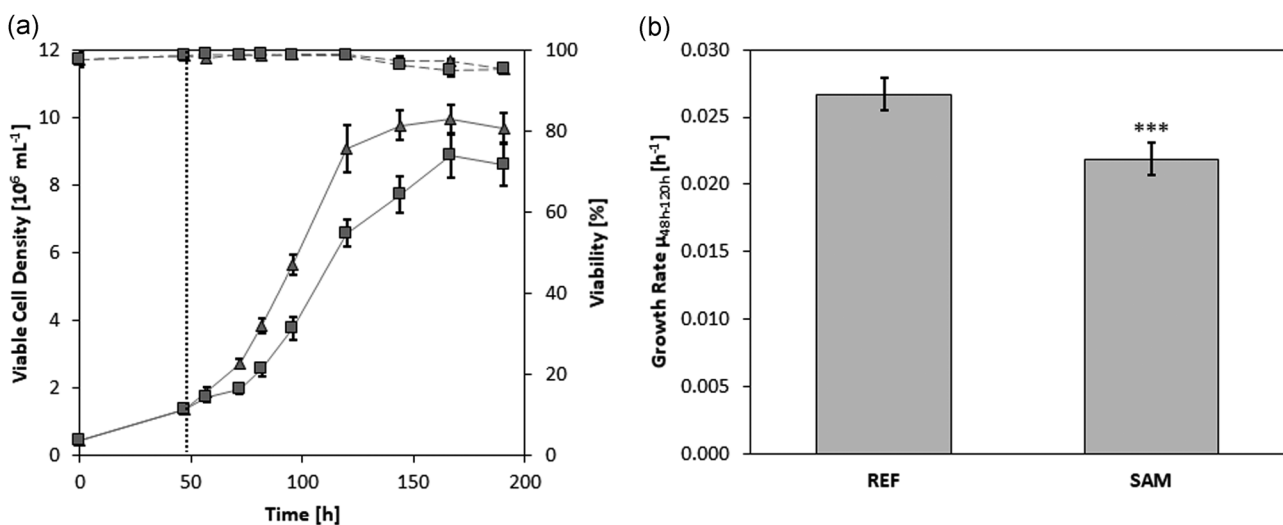

FIGURE 1 (a) Time courses of viable cell density (10^6/ml) and viability (%) of S-(5′-adenosyl)-L-methionine (SAM) supplemented cells (□) and reference (REF, Δ). SAM was added at 48 hr cultivation time. (b) Growth rate per hour (hr^{-1}) regarding the time interval 48–120 hr. Error bars show standard deviations of biological quadruplicates and technical replicates. Significance was tested with one-sided t-test. ***p = .001
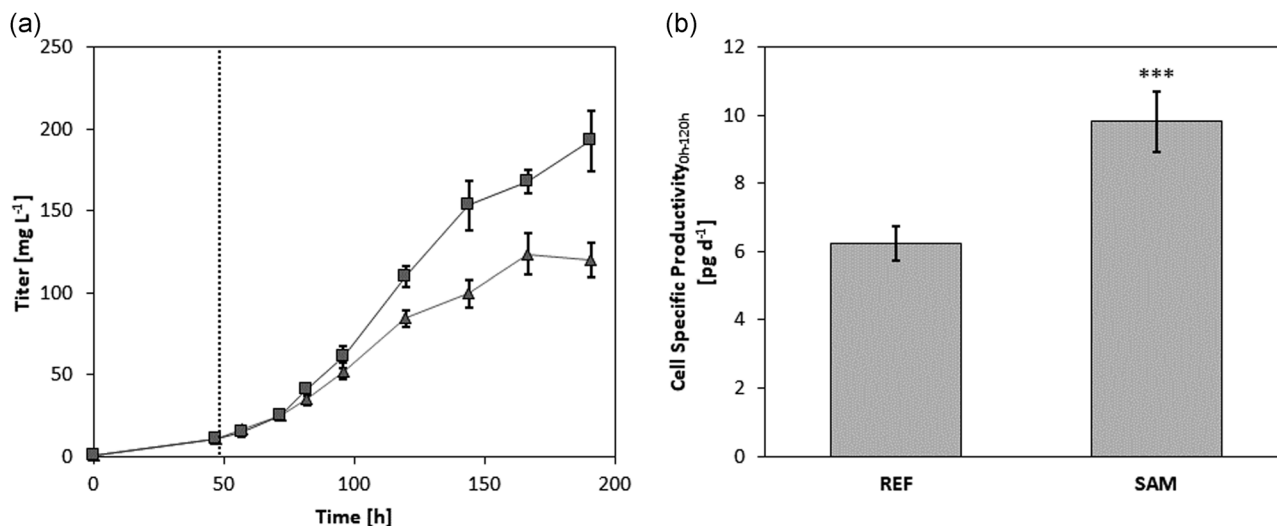
FIGURE 2 (a) Time courses of the antibody titer (mg/L) of S-(5′-adenosyl)-L-methionine (SAM) supplemented cells (□) and reference (REF, Δ). SAM was added after 48 hr cultivation time. (b) Cell specific productivity (pg/day) for the time interval 0–120 hr. Error bars show standard deviations of biological quadruplicates and technical replicates. Significance was tested with one-sided t-test. ***p = .001
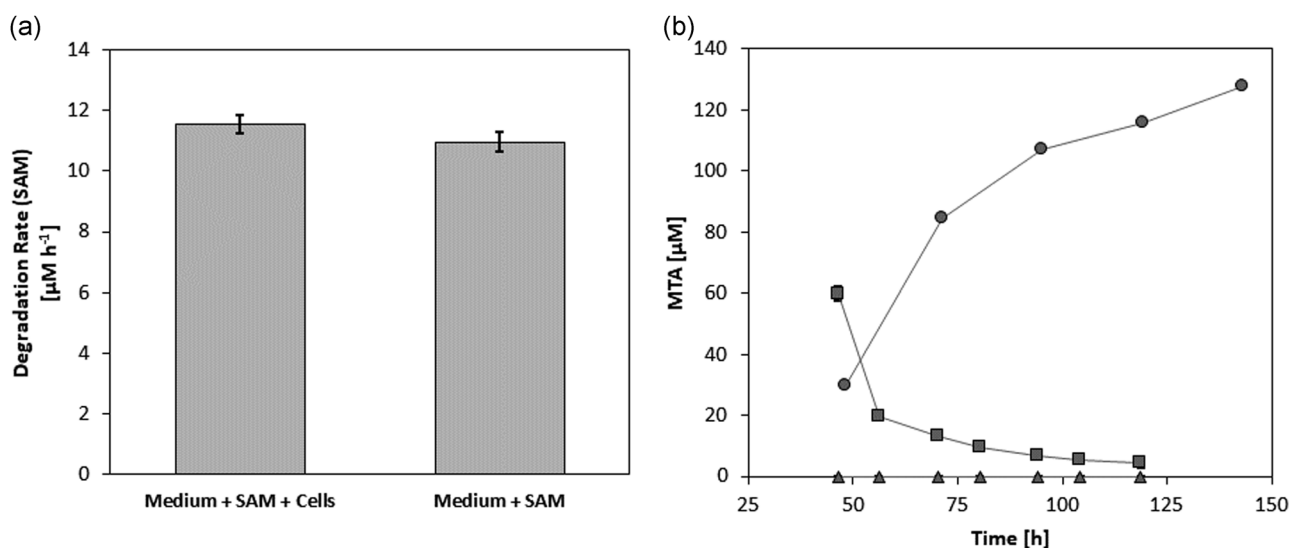

FIGURE 3 (a) Degradation rate (µM/hr) of S-(5′-adenosyl)-L-methionine (SAM) in medium at 37°C, 5% CO_2, and 150 rpm with and without cells. (b) Time courses of 5′-(methylthio)adenosine (MTA) concentration (µM) in the medium of SAM supplemented cells (□), reference (REF, Δ) and medium + SAM without cells (○). Error bars show standard deviations of biological duplicates

Accordingly, CSPs (Figure 5) of the first 120 hr revealed increased CSPs after the addition of SAM or MTA (SAM: 11.02 ± 1.70 pg/day and MTA: 8.73 ± 0.20 pg/day). These values corresponded to a 27–60% surplus of production. For comparison, HSL addition did not have an influence compared with the reference (HSL: 7.15 ± 0.64 pg/day and REF 6.87 ± 0.43 pg/day).

3.4 | SAM and MTA interact with the cell cycle

Propidium iodide staining revealed differences in the cell cycle phase distribution (Figure 6). All cells started from a common preculture that was split after 48 hr cultivation before adding SAM, MTA, HSL, or water (REF) as described above. About 12 hr after addition (60 hr cultivation time) SAM supplemented cells accumulated in G2-phase whereas MTA supplemented cells showed an increase in S-phase compared with the reference. Noteworthy, both cultures reduced the fraction of cells in G1-phase. Cells supplemented with HSL behaved like the reference. 12 hr later (72 hr cultivation time), the scenario of SAM-treated cultures had changed. Now, the fraction of cells in G1-phase was even higher than that in G2-phase compared with the reference. Still, MTA-treated cultures revealed alleviated numbers of cells in S-phase and less in G1-phase. After additional 12 hr (84 hr
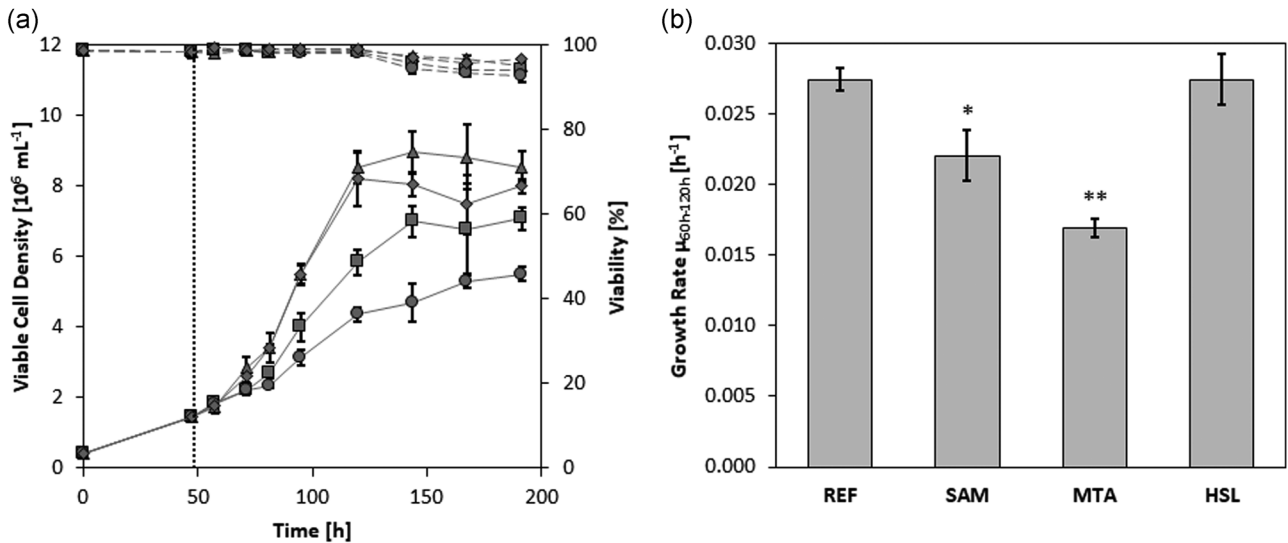
FIGURE 4 (a) Time courses of viable cell density (10^6/ml) and viability (%) of S-(5′-adenosyl)-L-methionine (SAM, □), 5′-(methylthio) adenosine (MTA, ○), and L-homoserine lactone hydrochloride (HSL, ◊) supplemented cells compared with the reference (REF, Δ). SAM, MTA, or HSL was added at 48 hr. (b) Growth rate (hr^{-1}) regarding the time interval 60–120 hr. Error bars show standard deviations of biological duplicates and technical replicates. Significance was tested with one-sided t-test. **p = .01, *p = .05

cultivation time) S-phase differences leveled out. Cells that were supplemented with SAM or MTA had more cells in G1-phase but less in G2-phase than the reference.

Additionally, the average cell diameter of all cultures was monitored. Cells supplemented with SAM or MTA revealed a rising average cell diameter of about 10% (SAM + 11.66%; MTA + 13.90%) 36 hr after addition. However, cell size was reduced to the size of the reference culture in the later phase of the cultivation.

4 | DISCUSSION

We added SAM to the medium of CHO cells to interact with the cellular metabolism and with SAM mediated regulation (Finkelstein, 1990; Mato et al., 1997). Clearly, SAM addition decreased the growth rate (Figure 1) which is in agreement with previous findings in liver cells (Cai et al., 1998; Pascale et al., 1993). It may be anticipated that changes in the DNA methylation pattern caused the growth phenotype
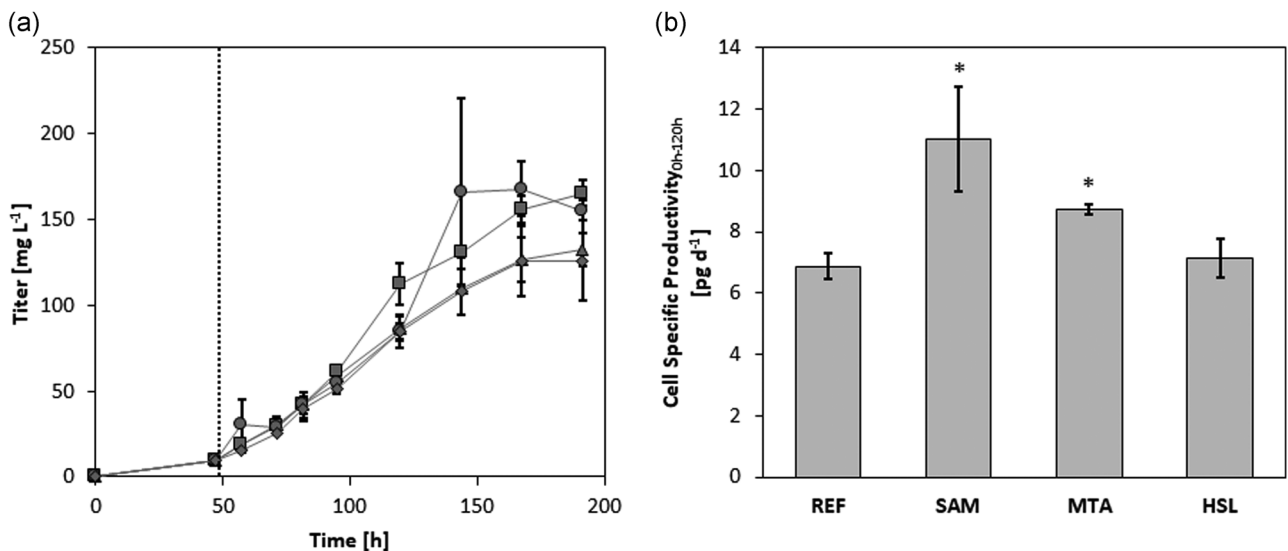

FIGURE 5 (a) Time courses of antibody titers (mg/L) of S-(5′-adenosyl)-L-methionine (SAM, □), 5′-(methylthio)adenosine (MTA, ○), and L-homoserine lactone hydrochloride (HSL, ◊) supplemented cells compared with the reference (REF, Δ). SAM, MTA, or HSL was added after 48 hr cultivation. (b) Cell specific productivity (pg/day) regarding the time interval 0–120 hr. Error bars show standard deviations of biological duplicates and technical replicates. Significance was tested with one-sided t-test. *p = .05
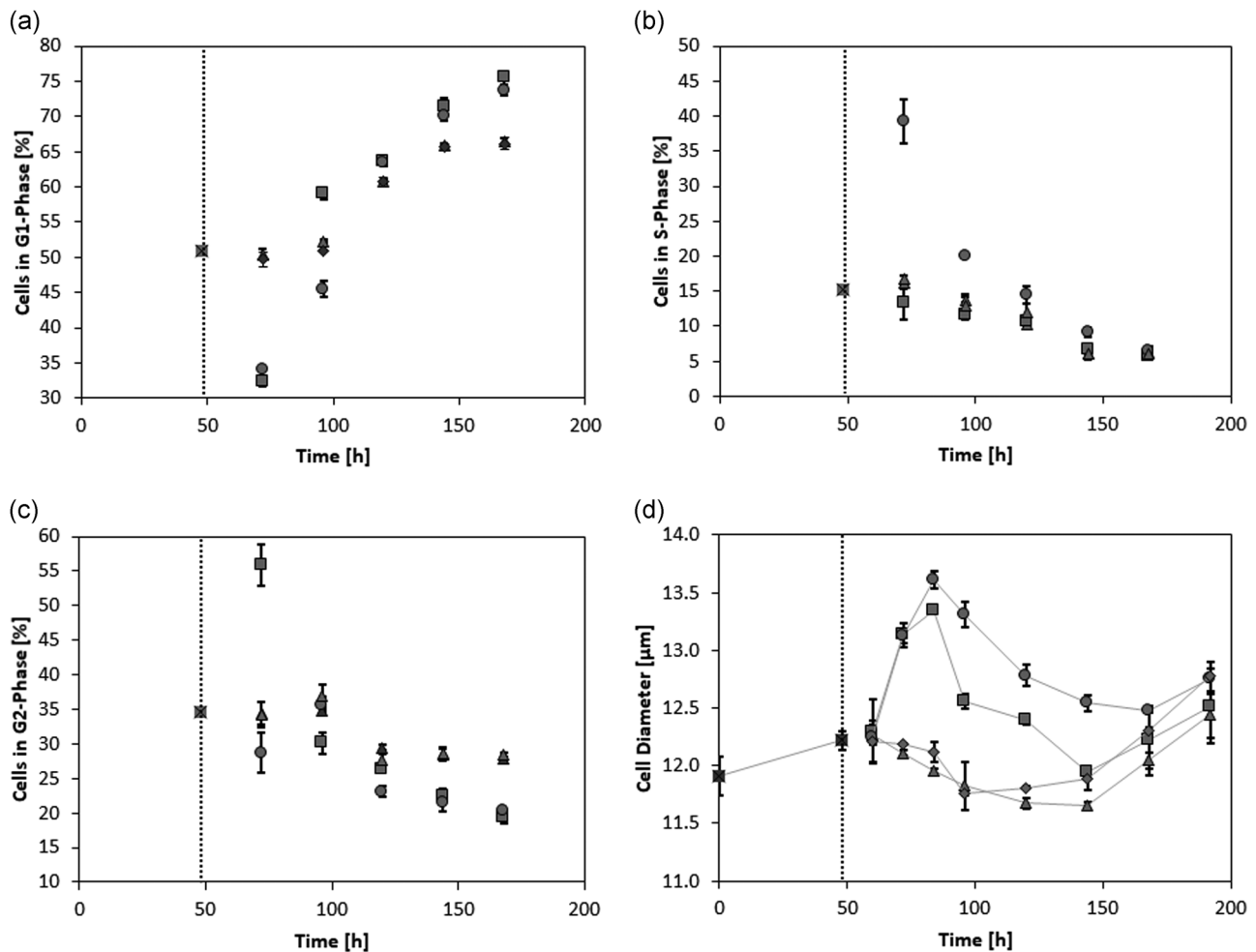
FIGURE 6 (a–c) Time courses of cell cycle phase distribution (%) and (d) average cell diameter (µm) of S-(5′-adenosyl)-L-methionine (SAM, ☐), 5′-(methylthio)adenosine (MTA, ○), and L-homoserine lactone hydrochloride (HSL) supplemented cells (◊) compared with the reference (REF, Δ) and common preculture (crossed ☐). Error bars show standard deviations of biological duplicates and technical replicates

(Feichtinger et al., 2016). Unfortunately, the identification of methylation differences with and without SAM addition was not manageable within the scope of the study.

Significantly increased CSP was found in CHO-DP12 cells after SAM addition (Figure 2), although growth rates were reduced. Metabolically, this phenomenon may be understood by assuming that SAM enters the cell boosting the precursor supply of the SAM cycle and/or alleviating the ATP dependent recycling. Mato et al. (1997) anticipated that liver cells take up extracellular SAM. The hypothesis was deduced from rising intracellular glutathione levels. However, Figure 3 reveals that decreasing extracellular SAM levels were observed irrespective of whether cells were present or not. Consequently, the cellular uptake of SAM is unlikely.

A computational study demonstrated that SAM degrades to MTA and HSL in water (Lankau, Kuo, & Yu, 2017). Consequently, we investigated the addition of these degradation products to the media. Whereas HSL did not create any particular phenotype, MTA caused effects very similar to the SAM addition (Figure 4). Noteworthy, MTA natively occurs in mammalian cells as part of the

polyamine biosynthesis (Pegg, 1988; Williams-Ashman, Seidenfeld, & Galletti, 1982). There, SAM is decarboxylated to MTA to access spermidine and spermine. Because high MTA levels inhibit polyamine synthesis MTA is rapidly degraded by 5′-methylthioadenosine phosphorylase. MTA was shown to permeate the cellular membrane. Furthermore, MTA was found to induce particular gene expression patterns, to regulate apoptosis, and to inhibit cell proliferation in hepatocytes, leukemia cells, fibroblasts, and lymphoma cells (Ansorena, 2002; Lee & Cho, 1998; Maher, 1993; Riscoe, Tower, & Ferro, 1984). The latter reflects the inhibition of polyamine synthesis by high MTA levels which reduces cell cycle progression in turn (Oredsson, 2003). Experiments with hepatic cells revealed inhibited DNA synthesis after MTA addition (Pascale, Simile, De Miglio, & Feo, 2002). The reduction of polyamine pathway intermediates such as spermidine after the addition of metabolic inhibitors induced arrest in the cell cycle's S-phase of CHO cells (Alm & Oredsson, 2000).

In agreement with this, we observed the accumulation of cells in S-phase after MTA addition concomitantly with a diminishing number in G1-phase compared with the REF (Figure 6). We hypothesize that

|

MTA inhibited polyamine synthesis finally creating the observed cytostatic effect (Subhi et al., 2003).

Both, SAM and MTA additions increased CSPs of CHO-DP12 cells (Figure 5). One explanation could be that cell cycle arrest particularly boosted cellular production rates (Fox, Patel, Yap, & Wang, 2004; Hendrick et al., 2001; Kaufmann, Mazur, Fussenegger, & Bailey, 1999; Pfizenmaier et al., 2015). However, those improvements are neither necessarily nor exclusively linked to a single cell cycle phase. Instead, they may benefit from multiple phases (Aggeler, Kapp, Tseng, & Werb, 1982; Al-Rubeai & Emery, 1990; Kim, Kim, & Lee, 2014; Kubbies & Stockinger, 1990; Lloyd, Holmes, Jackson, Emery, & Al-Rubeai, 2000). Accordingly, one may argue whether the improvement of CSP mirrors the benefits of arresting the cell cycle alone. Lloyd et al. (2000) observed CSPs proportional to the cell volume investigating four different CHO cell lines. As cell volume and cell cycle status are linked too, unequivocal conclusions are hard to get. As a result, they concluded that rather cells in S- and G2/M-phase show improved cellular productivity than those in G1-phase. However, this statement somewhat contradicts the findings of other groups (Fox et al., 2004; Hendrick et al., 2001; Kaufmann et al., 1999; Pfizenmaier et al., 2015). In our studies, cell diameters rose after MTA and SAM addition (Figure 6) which agrees with the findings of Lloyd et al. (2000). Strictly speaking, the observation does not exclude potential beneficial effects resulting from cell cycle arrest. In general, cell cycle arrest allows cells to use more energy for recombinant antibody production because biomass formation is hampered (Fussenegger, Mazur, & Bailey, 1997).

Besides the consequences of MTA and SAM on cell cycle and diameter, MTA may interact with a lot of other cell mechanisms (Ansorena, 2002; Lee & Cho, 1998; Maher, 1993; Riscoe et al., 1984). For instance, MTA inactivates SAH hydrolase (Williams-Ashman et al., 1982) leading to increased SAH levels finally resulting in reduced DNA methylation (Iraburu et al., 2002). As methylation is a crucial part of epigenetic regulation (Feichtinger et al., 2016) affecting transcription too (Wippermann et al., 2015) further transcriptional regulation programs are likely to be activated as well. Consequently, the substrate MTA will be further investigated, and its balanced addition is expected to intensify its boosting capability and avoid potential negative effects.

5 | CONCLUSION

The study was motivated by the idea to identify novel, non-conventional media components as promising additives to boost CSPs showcasing IgG-1 formation with CHO-DP12 cells. Testing the methyl group donor SAM, a multilevel effector was selected that may interact with different hierarchy levels of cellular regulation concomitantly. SAM addition improved CSPs by approx. 50% arresting the cell cycle and reducing cellular growth at the same time. A similar phenotype occurred when MTA was added which turned out to be the real effector resulting from SAM degradation and can transfer the cellular membrane.

The underlying mechanisms why CSPs are improved are not fully elucidated yet. However, the observations of cell cycle arrest and rising cell volumes support current state-of-the-art understanding but do not disclose key benefits in detail. Further metabolic and transcriptional studies are needed that are beyond the scope of this contribution. Nevertheless, the identification of SAM and MTA as promising media additives to boost CSPs may open the door for the search of other beneficial compounds that trigger cellular performance on multiple levels of metabolism and control.

CONFLICT OF INTERESTS

The authors declare that there are no conflict of interests.

ORCID

Natascha Verhagen 🄳 http://orcid.org/0000-0001-9604-8815
Ralf Takors 🄳 http://orcid.org/0000-0001-5837-6906

REFERENCES

Aggeler, J., Kapp, L., Tseng, S., & Werb, Z. (1982). Regulation of protein secretion in Chinese hamster ovary cells by cell cycle position and cell density. *Experimental Cell Research*, 139(2), 275–283. https://doi.org/10.1016/0014-4827(82)90252-X

Alm, K., & Oredsson, S. M. (2000). The organization of replicon clusters is not affected by polyamine depletion. *Journal of Structural Biology*, 131(1), 1–9. https://doi.org/10.1006/jsbi.2000.4263

Al-Rubeai, M., & Emery, A. N. (1990). Mechanisms and kinetics of monoclonal antibody synthesis and secretion in synchronous and asynchronous hybridoma cell cultures. *Journal of Biotechnology*, 16(1–2), 67–85. https://doi.org/10.1016/0168-1656(90)90066-K

Ansorena, E. (2002). S-adenosylmethionine and methylthioadenosine are antiapoptotic in cultured rat hepatocytes but proapoptotic in human hepatoma cells. *Hepatology*, 35(2), 274–280. https://doi.org/10.1053/jhep.2002.30419

Becker, M., Junghans, L., Teleki, A., Bechmann, J., & Takors, R. (2019). Perfusion cultures require optimum respiratory ATP supply to maximize cell-specific and volumetric productivities. *Biotechnology and Bioengineering*, 116(5), 951–960. https://doi.org/10.1002/bit.26926

Cai, J., Mao, Z., Hwang, J. J., & Lu, S. C. (1998). Differential expression of methionine adenosyltransferase genes influences the rate of growth of human hepatocellular carcinoma cells. *Cancer Research*, 58(7), 1444–1450.

Cantoni, G. L. (1951). Methylation of nicotinamide with soluble enzyme system from rat liver. *The Journal of Biological Chemistry*, 189(1), 203–216.

Dhiman, H., Gerstl, M. P., Ruckerbauer, D., Hanscho, M., Himmelbauer, H., Clarke, C., … Borth, N. (2019). Genetic and epigenetic variation across genes involved in energy metabolism and mitochondria of Chinese hamster ovary cell lines. *Biotechnology Journal*, 14(7), 1800681. https://doi.org/10.1002/biot.201800681

Feichtinger, J., Hernández, I., Fischer, C., Hanscho, M., Auer, N., Hackl, M., … Borth, N. (2016). Comprehensive genome and epigenome characterization of CHO cells in response to evolutionary pressures and over time. *Biotechnology and Bioengineering*, 113(10), 2241–2253. https://doi.org/10.1002/bit.25990

Feith, A., Teleki, A., Graf, M., Favilli, L., & Takors, R. (2019). Hilic-enabled 13c metabolomics strategies: Comparing quantitative precision and spectral accuracy of qtof high- and qqq low-resolution mass spectrometry. *Metabolites*, 9(4), https://doi.org/10.3390/metabo9040063

Finkelstein, J. D. (1990). Methionine metabolism in mammals. *The Journal of Nutritional Biochemistry*, 1(5), 228–237. https://doi.org/10.1016/0955-2863(90)90070-2

Fox, S. R., Patel, U. A., Yap, M. G. S., & Wang, D. I. C. (2004). Maximizing interferon-γ production by Chinese hamster ovary cells through temperature shift optimization: Experimental and modeling. *Biotechnology and Bioengineering*, 85(2), 177–184. https://doi.org/10.1002/bit.10861

Fussenegger, M., Mazur, X., & Bailey, J. E. (1997). A novel cytostatic process enhances the productivity of Chinese hamster ovary cells. *Biotechnology and Bioengineering*, 55(6), 927–939. https://doi.org/10.1002/(SICI)1097-0290(19970920)55:6<927::AID-BIT10>3.0.CO;2-4

Handlogten, M. W., Lee-O'Brien, A., Roy, G., Levitskaya, S. V., Venkat, R., Singh, S., & Ahuja, S. (2018). Intracellular response to process optimization and impact on productivity and product aggregates for a high-titer CHO cell process. *Biotechnology and Bioengineering*, 115(1), 126–138. https://doi.org/10.1002/bit.26460

Harreither, E., Hackl, M., Pichler, J., Shridhar, S., Auer, N., Łabaj, P. P., ... Borth, N. (2015). Microarray profiling of preselected CHO host cell subclones identifies gene expression patterns associated with increased production capacity. *Biotechnology Journal*, 10(10), 1625–1638. https://doi.org/10.1002/biot.201400857

Hendrick, V., Winnepenninckx, P., Abdelkafi, C., Vandeputte, O., Cherlet, M., Marique, T., ... Werenne, J. (2001). Increased productivity of recombinant tissular plasminogen activator (t-PA) by butyrate and shift of temperature: A cell cycle phases analysis. *Cytotechnology*, 36(1–3), 71–83. https://doi.org/10.1023/A:1014088919546

Hoffman, J. L. (1986). Chromatographic analysis of the chiral and covalent instability of S-adenosyl-L-methionine. *Biochemistry*, 25(15), 4444–4449. https://doi.org/10.1021/bi00363a041

Iraburu, M., García-Trevijano, E. R., Ansorena, E., Avila, M. A., Mato, J. M., Martínez-Chantar, M. L., ... Huang, Z. Z. (2002). S-adenosylmethionine and methylthioadenosine are antiapoptotic in cultured rat hepatocytes but proapoptotic in human hepatoma cells. *Hepatology*, 35(2), 274–280. https://doi.org/10.1053/jhep.2002.30419

Junghans, L., Teleki, A., Wijaya, A. W., Becker, M., Schweikert, M., & Takors, R. (2019). From nutritional wealth to autophagy: In vivo metabolic dynamics in the cytosol, mitochondrion and shuttles of IgG producing CHO cells. *Metabolic Engineering*, 54, 145–159. https://doi.org/10.1016/j.ymben.2019.02.005

Kaufmann, H., Mazur, X., Fussenegger, M., & Bailey, J. E. (1999). Influence of low temperature on productivity, proteome and protein phosphorylation of CHO cells. *Biotechnology and Bioengineering*, 63(5), 573–582. https://doi.org/10.1002/(SICI)1097-0290(19990605)63:5<573::AID-BIT7>3.0.CO;2-Y

Kim, W. H., Kim, Y. J., & Lee, G. M. (2014). Gadd45-induced cell cycle G2/M arrest for improved transient gene expression in Chinese hamster ovary cells. *Biotechnology and Bioprocess Engineering*, 19(3), 386–393. https://doi.org/10.1007/s12257-014-0151-0

Kubbies, M., & Stockinger, H. (1990). Cell cycle-dependent DHFR and t-PA production in cotransfected, MTX-amplified CHO cells revealed by dual-laser flow cytometry. *Experimental Cell Research*, 188(2), 267–271. https://doi.org/10.1016/0014-4827(90)90169-B

Lankau, T., Kuo, T. N., & Yu, C. H. (2017). Computational study of the degradation of S-adenosyl methionine in water. *The Journal of Physical Chemistry A*, 121(2), 505–514. https://doi.org/10.1021/acs.jpca.6b09639

Lee, S. H., & Cho, Y. D. (1998). Induction of apoptosis in leukemia U937 cells by 5′-deoxy-5′-methylthioadenosine, a potent inhibitor of protein carboxylmethyltransferase. *Experimental Cell Research*, 240(2), 282–292. https://doi.org/10.1006/excr.1998.4000

Lloyd, D. R., Holmes, P., Jackson, L. P., Emery, A. N., & Al-Rubeai, M. (2000). Relationship between cell size, cell cycle and specific recombinant protein productivity. *Cytotechnology*, 34(1–2), 59–70. https://doi.org/10.1023/A:1008103730027

Lu, S. C. (1998). Regulation of hepatic glutathione synthesis. *Seminars in Liver Disease*, 18(4), 331–343. https://doi.org/10.1055/s-2007-1007168

Maher, P. A. (1993). Inhibition of the tyrosine kinase activity of the fibroblast growth factor receptor by the methyltransferase inhibitor 5′-methylthioadenosine. *The Journal of Biological Chemistry*, 268(6), 4244–4249.

Mato, J., Alvarez, L., Ortiz, P., & Pajares, M. A. (1997). S-adenosylmethionine synthesis: Molecular mechanisms and clinical implications. *Pharmacology & Therapeutics*, 73(3), 265–280. https://doi.org/10.1016/S0163-7258(96)00197-0

Morana, A., Stiuso, P., Colonna, G., Lamberti, M., Rosa, M. De, & Cartenì, M. (2002). Stabilization of S-adenosyl-L-methionine promoted by trehalose. *Biochimica et Biophysica Acta*, 1573, 105–108.

Nematpour, F., Mahboudi, F., Khalaj, V., Vaziri, B., Ahmadi, S., Ahmadi, M., ... Davami, F. (2017). Optimization of monoclonal antibody expression in CHO cells by employing epigenetic gene regulation tools. *Turkish Journal of Biology*, 41(4), 622–628. https://doi.org/10.3906/biy-1702-18

Oredsson, S. M. (2003). Polyamine dependence of normal cell-cycle progression. *Biochemical Society Transactions*, 31(2), 366–370. https://doi.org/10.1042/BST0310366

Pascale, R. M., Simile, M. M., Seddaiu, M. A., Daino, L., Vinci, M. A., Pinna, G., ... Feo, F. (1993). Chemoprevention of rat liver carcinogenesis by S-adenosyl-L-methionine: Is DNA methylation involved? *Basic Life Sciences*, 61, 219–237. https://doi.org/10.1007/978-1-4615-2984-2_20

Pascale, R. M., Simile, M. M., De Miglio, M. R., & Feo, F. (2002). Chemoprevention of hepatocarcinogenesis: S-adenosyl-L-methionine. *Alcohol*, 27(3), 193–198. https://doi.org/10.1016/S0741-8329(02)00227-6

Pegg, A. E. (1988). Polyamine metabolism and its importance in neoplastic growth and as a target for chemotherapy. *Cancer Research*, 48(4), 759–774.

Pfizenmaier, J., Junghans, L., Teleki, A., & Takors, R. (2016). Hyperosmotic stimulus study discloses benefits in ATP supply and reveals miRNA/mRNA targets to improve recombinant protein production of CHO cells. *Biotechnology Journal*, 11(8), 1037–1047. https://doi.org/10.1002/biot.201500606

Pfizenmaier, J., Matuszczyk, J.-C., & Takors, R. (2015). Changes in intracellular ATP-content of CHO cells as response to hyperosmolality. *Biotechnology Progress*, 31(5), 1212–1216. https://doi.org/10.1002/btpr.2143

Pfizenmaier-Wu, J. I. (2017). *Metabolic and transcriptomic response to hyperosmotic stimulus reveals strategies for optimization of antibody producing Chinese hamster ovary cells*. University of Stuttgart. Retrieved from https://doi.org/10.18419/opus-9145

Reinhart, D., Damjanovic, L., Kaisermayer, C., & Kunert, R. (2015). Benchmarking of commercially available CHO cell culture media for antibody production. *Applied Microbiology and Biotechnology*, 99(11), 4645–4657. https://doi.org/10.1007/s00253-015-6514-4

Riscoe, M. K., Tower, P. A., & Ferro, A. J. (1984). Mechanism of action of 5′-methylthioadenosine in S49 cells. *Biochemical Pharmacology*, 33(22), 3639–3643. https://doi.org/10.1016/0006-2952(84)90150-3

Schaub, J., Clemens, C., Schorn, P., Hildebrandt, T., Rust, W., Mennerich, D., ... Schulz, T. W. (2010). CHO gene expression profiling in biopharmaceutical process analysis and design. *Biotechnology and Bioengineering*, 105(2), 431–438. https://doi.org/10.1002/bit.22549

Sha, S., Bhatia, H., & Yoon, S. (2018). An RNA-seq based transcriptomic investigation into the productivity and growth variants with Chinese hamster ovary cells. *Journal of Biotechnology*, 271(2010), 37–46. https://doi.org/10.1016/j.jbiotec.2018.02.008

Subhi, A. L., Diegelman, P., Porter, C. W., Tang, B., Lu, Z. J., Markham, G. D., & Kruger, W. D. (2003). Methylthioadenosine phosphorylase regulates ornithine decarboxylase by production of downstream metabolites. *Journal of Biological Chemistry*, *278*(50), 49868–49873. https://doi.org/10.1074/jbc.M308451200

Teleki, A., Sánchez-Kopper, A., & Takors, R. (2015). Alkaline conditions in hydrophilic interaction liquid chromatography for intracellular metabolite quantification using tandem mass spectrometry. *Analytical Biochemistry*, *475*, 4–13. https://doi.org/10.1016/j.ab.2015.01.002

Templeton, N., Smith, K. D., McAtee-Pereira, A. G., Dorai, H., Betenbaugh, M. J., Lang, S. E., & Young, J. D. (2017). Application of 13C flux analysis to identify high-productivity CHO metabolic phenotypes. *Metabolic Engineering*, *43*(December), 218–225. https://doi.org/10.1016/j.ymben.2017.01.008

Templeton, N., Xu, S., Roush, D. J., & Chen, H. (2017). 13C metabolic flux analysis identifies limitations to increasing specific productivity in fed-batch and perfusion. *Metabolic Engineering*, *44*(September), 126–133. https://doi.org/10.1016/j.ymben.2017.09.010

Walsh, G. (2018). Biopharmaceutical benchmarks 2018. *Nature Biotechnology*, *36*(12), 1136–1145. https://doi.org/10.1038/nbt.4305

Williams-Ashman, H. G., Seidenfeld, J., & Galletti, P. (1982). Trends in the biochemical pharmacology of 5′-deoxy-5′-methylthioadenosine. *Biochemical Pharmacology*, *31*(3), 277–288. https://doi.org/10.1016/0006-2952(82)90171-X

Wippermann, A., Rupp, O., Brinkrolf, K., Hoffrogge, R., & Noll, T. (2015). The DNA methylation landscape of Chinese hamster ovary (CHO) DP-12 cells. *Journal of Biotechnology*, *199*, 38–46. https://doi.org/10.1016/j.jbiotec.2015.02.014

Wurm, F. M. (2004). Production of recombinant protein therapeutics in cultivated mammalian cells. *Nature Biotechnology*, *22*(11), 1393–1398. https://doi.org/10.1038/nbt1026

Zhang, H., Wang, H., Liu, M., Zhang, T., Zhang, J., Wang, X., & Xiang, W. (2013). Rational development of a serum-free medium and fed-batch process for a GS-CHO cell line expressing recombinant antibody. *Cytotechnology*, *65*(3), 363–378. https://doi.org/10.1007/s10616-012-9488-4